Voltage-modulation of oxygen vacancy-related dipoles in gate insulators as a mechanism for non-volatile memories

J. Cuesta-Lopez*, E.G. Marin, A. Toral-Lopez, M.D. Ganeriwala, F.G. Ruiz, F. Pasadas, A. Godoy

Department of Electronics and Computer Technology, University of Granada, Granada 18071, Spain.
*e-mail: jcuesta@ugr.es

1. Abstract

We simulate voltage-driven ion migration in gate oxides as a potential mechanism to develop non-volatile memories (NVMs) as appropriate candidates for neuromorphic computing applications. Our study aims to give insights about the impact of ion mobility and ion concentration in the device memory window (MW).

2. Introduction

NVMs are attracting great interest as key components to implement highly efficient artificial neural networks (ANNs) [1]. In spite of some successful experimental examples [2,3], the fabrication of NVMs is still in an early stage of development, with most demonstrations exploiting filamentary formation, a physical process prone to statistical fluctuations. In this context, NVMs based on three terminal transistors, exploiting the voltage-driven migration of oxygen vacancies and ions in the gate-insulator stack, constitute a promising alternative. In this work, we implement an *ad-hoc* simulator to analyze the impact that mobility and concentration of oxygen vacancy-related dipoles have in the performance of these devices.

3. Methods

The simulated device consists of a 20 nm-thick Ge channel sandwiched between two layers of Al_2O_3. The schematic with geometrical specifications and material parameters are shown in **Fig. 1** and **Table 1**, respectively. The 3.5 nm-thick top oxide contains mobile oxygen ions ($z = -2$) and oxygen vacancies ($z = +2$), where z is the ion valence. At a sufficiently large gate bias (V_{fg}), mobile ions drift, modifying the threshold voltage (V_{th}) and, subsequently, the channel conductivity. Simulations are performed using an in-house numerical tool that self-consistently solves the two-dimensional Poisson equation, the continuity equation for electrons and holes based on the pseudo-Fermi energy level, and the drift-diffusion equation for ions. The applied signals are divided in two categories as shown in **Fig. 2**: (i) a Program/Erase (P/E) signal, and (ii) a Read signal. The P/E signal is a 100 ns wide square pulse with amplitude $V_{fg} = +4/-4$ V at constant $V_{ds} = 0$ V to separate the mobile ions inside the top gate oxide. The read process makes use of triangular signals with amplitude $V_{fg} = 0.5$ V and frequency 10 MHz, at a constant $V_{ds} = -50$ mV. This reading signal barely perturbs the ion distribution set in the P/E phase. As a result, the application of the P/E pulses produces transfer characteristics with different threshold voltages as depicted in **Fig. 3**. The device memory window (MW) is defined as the difference between the V_{fg} required to get the drain current density $J = -0.5$ µA/µm after the application of P/E pulses.

4. Results and Conclusions

The MW is affected by ion mobility, μ_c, and ion concentration, c_0. It was found that a high value of both parameters is required to achieve a large MW, as depicted in **Fig. 4** and **Fig. 5**. However, if these parameters are excessively high, ions will follow the input triangular signal without delay or the switchable polarization would be reduced, narrowing the MW in the reading process. On the contrary, if μ_c and c_0 are too low, ions will not drift during the P/E process or would not significantly impact the channel electrostatics regardless their distribution. In both cases, the MW will be reduced. Another important metric to consider is the stability of the MW, which tends to reduce after several reading cycles for the higher μ_c and c_0 values, as shown in **Fig. 6**. It is concluded that only for a limited range of values, both parameters provide the required performance. In this study, the optimal MW is achieved for $\mu_c = 7.2 \cdot 10^{-10}$ cm^2/(Vs), $c_0 = 9.5 \cdot 10^{20}$ cm^{-3}.

5. Acknowledgements

This work is funded by the FEDER/Junta de Andalucía through the projects A-TIC-646-UGR20 and P20-00633, and the Spanish Government MCIN/AEI/10.13039/501100011033 through the projects PID2020-116518GB-I00 and TED2021-129769B-I00 (NextGenerationEU/PRTR). F. Pasadas acknowledges funding from PAIDI 2020 and the European Social Fund Operational Programme 2014–2020 no. 20804. J. Cuesta-Lopez acknowledges the FPU program FPU019/05132, and M.D. Ganeriwala the EU through project H2020-MSCA-IF 2020.

References

[1] S. Brivio et al., Neuromorph. Comput. Eng., vol. 2, pp. 1-22, 2022. https://doi.org/10.1088/2634-4386/ac9012

[2] Y. Peng et al., Nanoscale Res. Let., vol. 15:134, pp. 1-6, 2020. https://doi.org/10.1186/s11671-020-03364-3

[3] Z. Feng et al., Adv. Electron. Mater, vol. 2100414, pp. 1-8, 2021.https://doi.org/10.1002/aelm.202100414

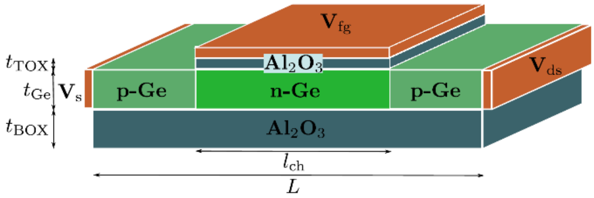

Fig. 1. Device structure employed in this study.

t_{TOX} = 3.5 nm	t_{Ge} = 20 nm	t_{BOX} = 20 nm
L = 200 µm	l_{ch} = 100 nm	V_{s} = 0 V
μ_{n} = 3900 cm^2/(Vs)	μ_{p} = 1900 cm^2/(Vs)	f = 10 MHz
$\varepsilon_{\mathrm{Ge}} = 16\varepsilon_0$	$\varepsilon_{\mathrm{ox}} = 10\varepsilon_0$	$z = \pm 2$
$N_{\mathrm{A}} = 10^{17}$ cm^{-3}	$N_{\mathrm{D}} = 10^{15}$ cm^{-3}	

Table 1. Geometrical and material parameters employed in the device simulation.

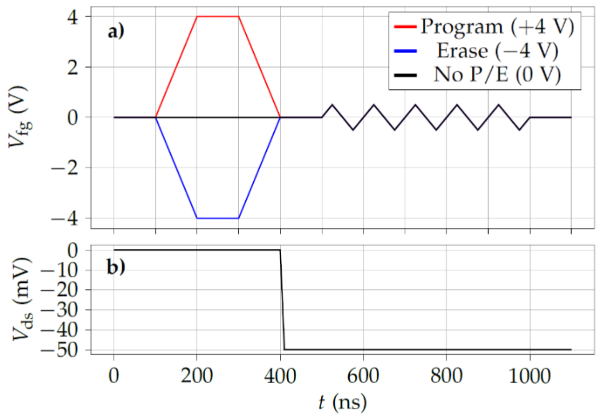

Fig. 2. Voltage signals applied to (a) the front gate terminal V_{fg}, and (b) the drain contact, V_{ds}.

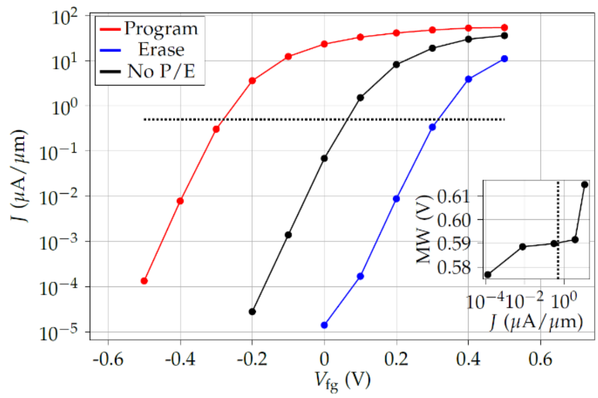

Fig. 3. Current densities obtained for the sweep-down of the first Reading pulse after a Program signal (red, +4V), an Erase signal (blue, -4V) and a neutral signal (black, 0V). These results correspond to parameters $\mu_c = 7.2 \cdot 10^{-10}$ cm^2/(Vs), $c_0 = 9.5 \cdot 10^{20}$ cm^{-3}. The inset depicts the Memory Window (MW) as a function of current density, J (µA/µm), with dotted line at J = 0.5 µA/µm.

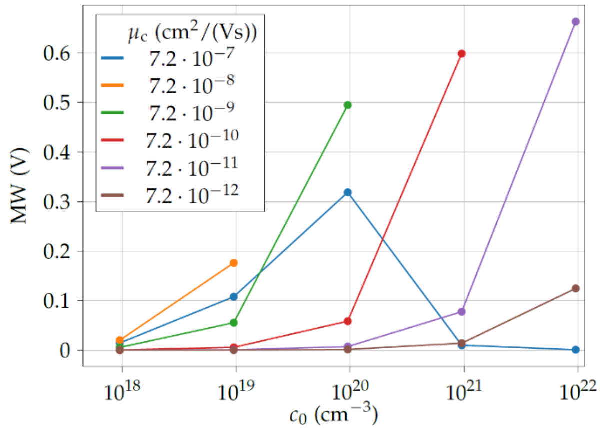

Fig. 4. MW as a function of c_0, measured in the sweep-down of the first cycle, for different values of μ_c.

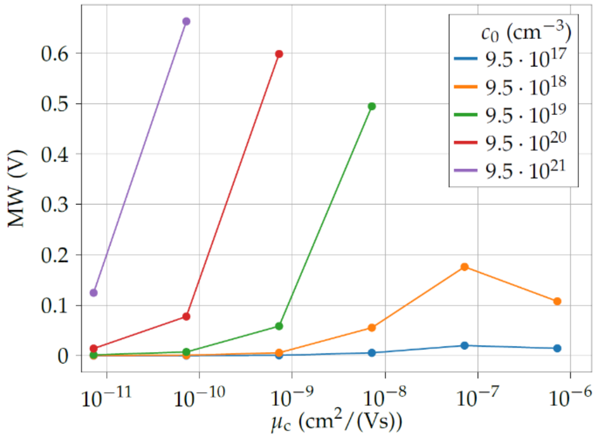

Fig. 5. MW as a function of μ_c, measured in the sweep-down of the first cycle, for different values of c_0.

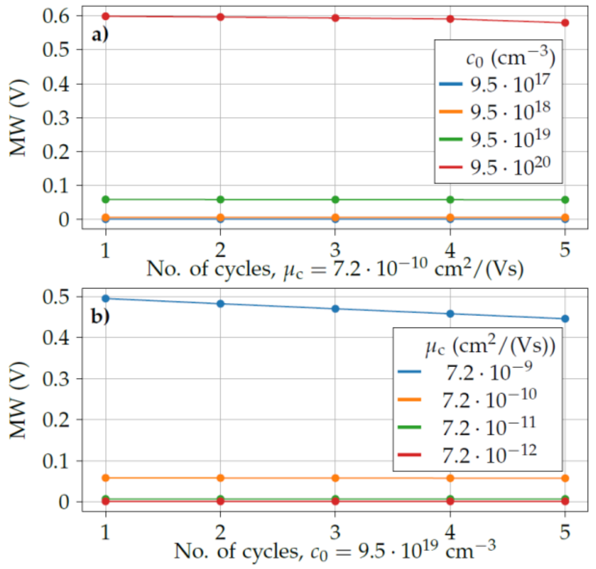

Fig. 6. MW measured during the sweep-down of each cycle for (a) $\mu_c = 7.2 \cdot 10^{-10}$ cm^2/(Vs) and (b) $c_0 = 9.5 \cdot 10^{19}$cm^{-3} varying c_0 and μ_c, respectively.